

Highly Sensitive Electrochemical Cholesterol Biosensor based on Graphene-ZnS Modified Carbon Paper Electrode

G. Suganthi ^a, G. Amirtha Varshini ^{a,*}

^a Department of Physics, Guru Nanak College, Chennai, Tamil Nadu, India

* Corresponding author Email: amirthavarshinigovindarajan@gmail.com

DOI: <https://doi.org/10.54392/nxxt2441>

Received: 31-07-2024; Revised: 10-11-2024; Accepted: 18-11-2024; Published: 27-11-2024

Abstract: In this study, we present a new and straightforward graphene-zinc sulfide (ZnS) nanocomposite that we've successfully created for use in a carbon paper-based cholesterol biosensor. By integrating ZnS nanoparticles onto graphene sheets, we've significantly enhanced the electrocatalytic performance of the electrode, which boosts the sensitivity of the cholesterol biosensor. We carried out a comprehensive analysis of the nanocomposite's structure and components using techniques like XRD, SEM, and TEM. For detecting cholesterol, we immobilized cholesterol oxidase onto the ZnS/G modified carbon paper electrode. Our cyclic voltammetry (CV) analysis indicated that there's direct electron transfer happening between the enzyme and the electrode. The biosensor we developed showcased a quick response time, impressive sensitivity, a wide linear detection range, and a low detection limit. Plus, the ZnS/G modified carbon paper electrode proved to be highly selective, consistently reproducible, and stable for over a month.

Keywords: ZnS, Biosensor, Nanoparticles, XRD, SEM, TEM

1. Introduction

Assessing cholesterol levels in human blood is really important for clinical analysis. High cholesterol in blood serum is closely associated with several serious health issues, such as heart disease, coronary artery disease, high blood pressure, cerebral thrombosis, and arteriosclerosis, which are all considered major medical conditions [1, 2]. Therefore, the regular assessment of cholesterol levels has been a subject of extensive research in clinical diagnostics. Conventional analytical techniques such as colorimetric assays, spectrophotometry, and HPLC have been developed for cholesterol quantification [3, 4]. However, these traditional methodologies suffer from limitations due to their time-consuming nature and complex procedures. As a promising alternative, numerous researchers are exploring the development of electrochemical methods. Electrochemical biosensors, in theory, offer accuracy, cost-effectiveness, efficiency, sensitivity, rapid results, and objective data. Fundamentally, these electrochemical biosensors operate based on the principle of cholesterol oxidase (ChOx) immobilization on the electrode surface [5, 6].

A wide variety of electrode devices are currently available. Paper-based devices are particularly notable for their versatility due to their

ultra-low material cost, ease of use, and potential for storage, making them promising, economical, and biocompatible materials for biosensor fabrication [7, 8]. Additionally, the porous fiber network of paper facilitates capillary flow, allowing for fluid sample movement without the need for active pumping.

Toray's conducting carbon paper is commonly used as a diffusion layer in fuel cells, supercapacitors, and batteries. This popularity stems from its impressive mechanical strength, conductivity, large surface area, and excellent gas permeability [9, 10]. Additionally, Toray carbon paper offers features like easy handling, high electrochemical stability, and low electrical resistivity, making it a great choice for developing working electrodes in biosensors [11, 12].

In recent years, graphene has really caught the eye of researchers due to its unique two-dimensional honeycomb structure, which consists of a single layer of carbon atoms [13, 14]. Its growing popularity spans several fields, including biosensors, molecular resolution sensors, energy storage and conversion, ultrafast electronics, and drug delivery. This surge in interest is largely due to graphene's impressive specific surface area, outstanding electrical and thermal conductivities, affordability, good



biocompatibility, and remarkable mechanical strength [15, 16].

Zinc sulfide (ZnS) nanoparticles are another fascinating material that boasts remarkable properties, making them incredibly useful in a range of applications like biosensor manufacturing, cell imaging, and electrical materials. Additionally, ZnS is particularly well-suited for creating enzymatic sensors because of its excellent chemical stability, biocompatibility, high electron transfer rates, and non-toxic nature [17, 18].

Nanocomposites that integrate metal nanoparticles with exfoliated graphene nanosheets present notable benefits for biosensor applications. These benefits include a larger effective surface area for better enzyme loading, improved biocompatibility, and enhanced electrical conductivity, all of which contribute to the development of highly sensitive devices [19, 20]. Enzyme immobilization generally relies on methods such as covalent attachment, adsorption, cross-linking, and entrapment. Covalent attachment and cross-linking are often favored over physical adsorption due to their effectiveness in preventing enzyme leaching from the sensor surface. Electrochemical sensors based on carbon paper have attracted considerable interest because of their simple fabrication, inherent liquid absorbency, flexibility, ready availability, and low cost. Therefore, this work aims to develop a straightforward and sensitive cholesterol biosensor.

This study reports on an efficient biosensor for cholesterol detection, utilizing a graphene-zinc sulfide nanoparticle (G-ZnS) modified carbon paper electrode. The synthesized G-ZnS material was characterized using various techniques and subsequently employed as a robust transducer for both hydrogen peroxide (H_2O_2) and enzymatic cholesterol electrochemical detection. The biosensor demonstrated enhanced catalytic properties compared to a sensor using only a ZnS matrix. This improvement is attributed to the interaction between ZnS and the graphene support, which facilitates better enzyme adhesion and stability, resulting in a rapid biosensor response.

2. Experimental

2.1. Chemicals and Reagents

Cholesterol, Triton X-100, cholesterol oxidase, flake graphite powder (99.99% SP-1, Bay Carbon, with an average particle size of 45 μm), zinc chloride ($ZnCl_2$), and sodium sulfide (Na_2S) were acquired from Sigma Aldrich. Carbon paper (TGP H-60) was obtained

from Toray Industries. Hydrogen peroxide (H_2O_2 , 30% wt/V) was sourced from Fisher Scientific. Concentrated sulfuric acid (H_2SO_4 , 99%), concentrated nitric acid (HNO_3 , 98%), and potassium permanganate ($KMnO_4$) were supplied by Rankem Chemicals, India, and were used as received without further purification. A 0.1 M potassium phosphate buffer solution (PBS, pH 7) was prepared utilizing dipotassium hydrogen phosphate (K_2HPO_4) and sodium dihydrogen phosphate (K_2HPO_4). All chemicals employed were of analytical grade. Deionized (DI) water was utilized for all electrochemical experiments and synthesis procedures.

2.2. Characterization and Measurement

X-ray Diffraction (XRD) analysis was conducted using a PANalytical X'Pert Pro diffractometer equipped with Cu-K α radiation to assess the crystallinity of the samples. To identify functional groups, Fourier Transform Infrared (FTIR) spectroscopy was performed across a spectral range of 100–4000 cm^{-1} . Cyclic voltammetry (CV) experiments were carried out with a CH Instruments CHI 608C electrochemical analyzer, which utilized a three-electrode setup comprising an Ag/AgCl reference electrode, a platinum (Pt) counter electrode, and working electrodes made from ZnS/G modified carbon paper. Additionally, surface morphology and structural characteristics were examined using Scanning Electron Microscopy (SEM) with an FEI Quanta 3D instrument, and Transmission Electron Microscopy (TEM) with a TECNAI G² F20 S-TWIN instrument.

2.3. Preparation of Graphene sheets (G)

A modified Hummer's approach was utilized to produce graphene oxide (GO) from graphite powder. The process began by combining 1 g of graphite with 0.5 g of sodium nitrate. Following this, 23 ml of concentrated sulfuric acid was cautiously incorporated into the mixture while maintaining continuous stirring. After a reaction time of one hour, 3 g of potassium permanganate ($KMnO_4$) was slowly added to the solution, ensuring that the temperature remained below 20 $^{\circ}\text{C}$ to mitigate the risk of exothermic reactions. The reaction mixture was then stirred at 35 $^{\circ}\text{C}$ for a period of 12 hours, after which it was diluted with 500 ml of water while stirring vigorously. To achieve complete oxidation by $KMnO_4$, the suspension was treated with 5 ml of a 30% hydrogen peroxide (H_2O_2) solution. The resultant mixture was subjected to washing with hydrochloric acid (HCl) followed by water, and then underwent filtration and drying to obtain



graphene oxide (GO) sheets. Subsequently, thermal exfoliation was applied to convert the synthesized GO into graphene sheets. This involved rapidly placing a quartz crucible containing GO into a muffle furnace set to 900 °C for 2 minutes in an air atmosphere. Finally, to promote the dispersion of metal nanoparticles onto the graphene surface, the prepared graphene (G) was functionalized by stirring continuously in a 3:1 mixture of concentrated sulfuric acid and nitric acid for 30 minutes.

2.4. Preparation of G/ZnS nanocomposites

A modified Hummer's method was used to synthesize graphene, after which ZnS nanoparticles were deposited using chemical reduction. Typically, 0.1 g of graphene was dispersed in deionized water and then treated with a 1M zinc chloride solution. The resulting mixture was magnetically stirred for 12 hours. Subsequently, nanocrystalline ZnS particles were deposited onto the graphene sheets by employing a reducing solution of 1M sodium sulfide. The final suspension was washed, filtered, and then dried at 60°C after the reaction completion.

2.5. Fabrication of G/ChOx/CP and G/ZnS/ChOx/CP electrodes

A carbon paper electrode (CPE) served as the base for the development of the bioelectrode. The modification of the CPE was accomplished using a simple drop-casting technique. Initially, 1 mg of graphene (G) was subjected to sonication in 1 ml of a 0.5% Nafion solution, which aids in enhancing the dispersion and stability of the graphene material. Subsequently, 15 µl of this graphene solution was applied to the surface of the CPE via drop-casting and allowed to dry at ambient temperature. Additionally, a G/ZnS@CPE electrode was fabricated for comparative analysis, utilizing the same weight ratios of materials as those in the G@CPE electrode. To complete the bioelectrode fabrication, 10 µl of a cholesterol oxidase (ChOx) enzyme solution was drop-cast onto the graphene-modified CPE. The enzyme-modified electrode was then dried and stored at 4 °C to maintain the enzyme's activity. Figure 1 illustrates the steps involved in the preparation of electrodes with nanocomposite.

2.6. Preparation of Solutions

Cholesterol was solubilized in deionized water using 10% Triton X-100 to formulate a stock solution,

which was then refrigerated at 4°C for storage. This stock solution was further diluted to produce a series of solutions with different cholesterol concentrations. Additionally, a 0.1 M potassium phosphate buffer solution (PBS, pH 7) was prepared by dissolving dipotassium hydrogen phosphate (K_2HPO_4) and sodium dihydrogen phosphate (KH_2PO_4) in deionized water.

3. Results and discussion

3.1 Material characterization

The characterization of G and ZnS/G nanocomposites were studied by XRD, FTIR, FESEM, TEM, EDX spectroscopy.

To analyze the structural changes, the X-ray Diffraction (XRD) pattern of the hybrid composite was compared with that of the initial starting material. Figure 2 illustrates the XRD patterns for (a) ZnS and (b) ZnS-G. For ZnS nanoparticles (Fig. 2a), well-resolved crystalline peaks are identified at 2θ values of 13.15°, 21.8°, 26.6°, 31.6°, 40.5°, and 55° [10]. Figure 2b reveals diffraction peaks for ZnS-G at 2θ values of 29.0°, 33.5°, 48.1°, and 57.0° (JCPDS No. 05-0566), which are characteristic of the ZnS nanostructure, alongside a peak corresponding to C (002). This indicates the effective decoration of graphene with ZnS nanoparticles.

Fourier Transform Infrared (FTIR) spectroscopy was employed to evaluate the compatibility of the materials, utilizing a Perkin Elmer FTIR spectrophotometer within the spectral range of 4000 to 500 cm^{-1} . Spectra were recorded and compared for zinc sulfide (ZnS), graphene, and their admixture. As shown in Figure 3b, the FTIR spectra demonstrate prominent bands at 643 cm^{-1} , 947 cm^{-1} , 1129 cm^{-1} , 1410 cm^{-1} , 1629 cm^{-1} , and 3419 cm^{-1} , which are characteristic of ZnS nanoparticles, consistent with literature reports [11]. The peak observed at 612 cm^{-1} is specifically assigned to the ZnS band, indicative of sulfide linkages. Furthermore, absorption bands associated with absorbed water, namely O-H bending and stretching modes, are identified at 1629 cm^{-1} and 3419 cm^{-1} , respectively. FT-IR spectroscopy, presented in Figure 3a, confirmed the successful functionalization of acid-oxidized graphene sheets, revealing the presence of several functional groups, particularly carbonyl and hydroxyl functionalities, as anticipated [13].

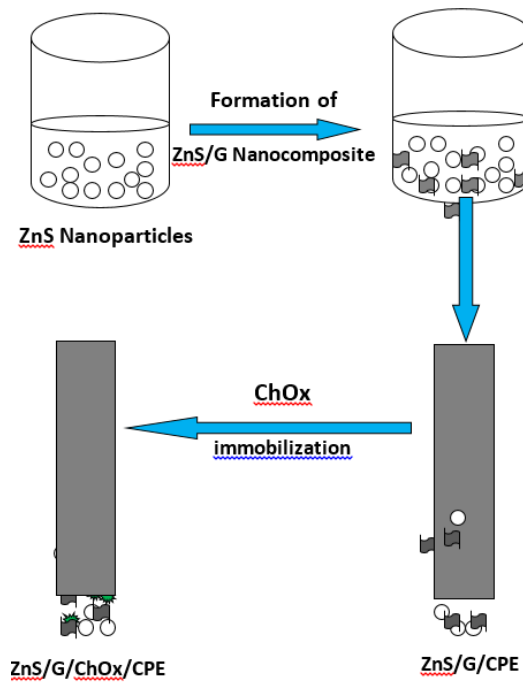
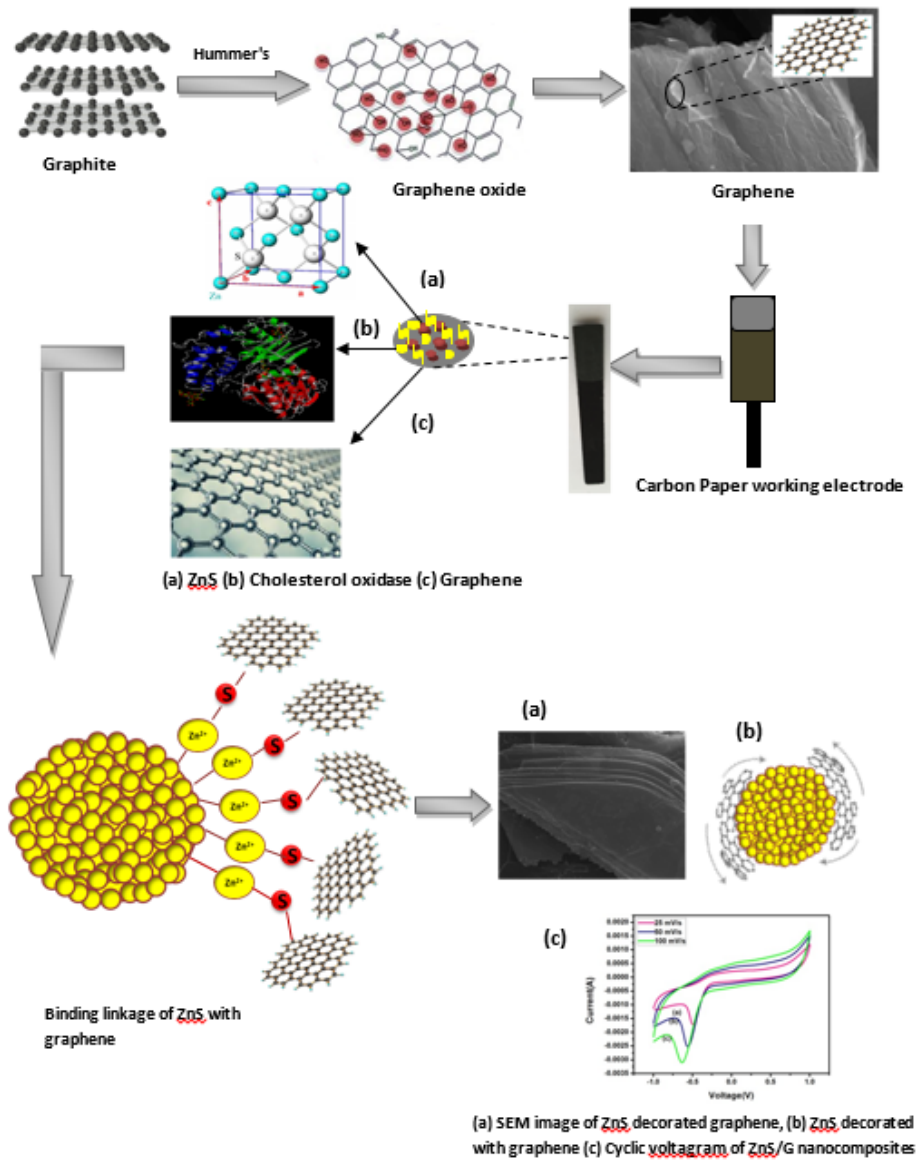


Figure 1. Schematic diagram showing the fabrication procedure of ZnS/CHI/ChOx/NA/CPE biosensor

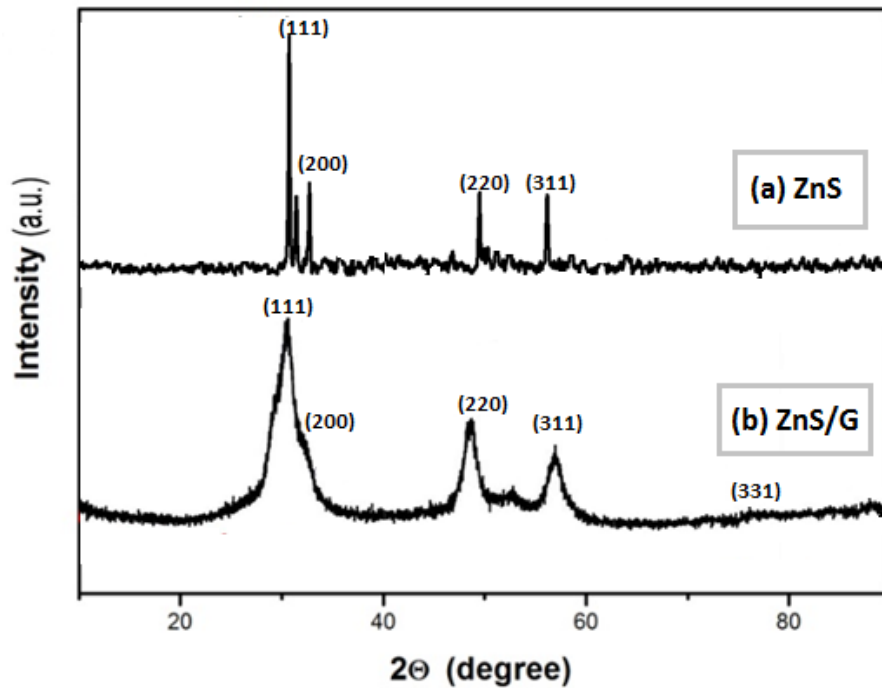


Figure 2. XRD of ZnS and ZnS/G

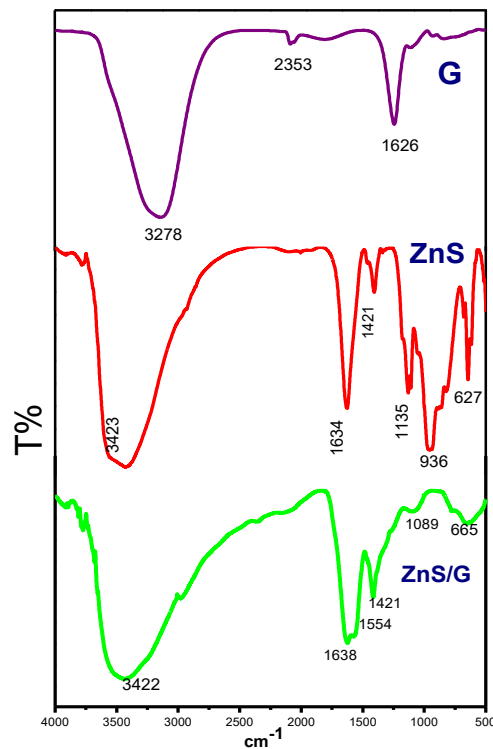


Figure 3. FTIR spectra for (a) G, (b) ZnS and (c) G/ZnS

To validate the formation of the desired surface functional groups on acid-oxidized graphene, surface characterization was performed using FT-IR spectroscopy. The absorption spectra exhibited characteristic peaks at 3441 cm^{-1} (OH stretching) and 1624 cm^{-1} (OH bending). Collectively, this FTIR

analysis indicates a homogeneous dispersion of ZnS nanoparticles across the graphene surface.

The morphology of the surface is crucial for assessing the electrochemical performance of the sensing material. To investigate this relationship, we

employed electron microscopy techniques to examine the surface characteristics of the sample more closely. The results from Scanning Electron Microscopy (SEM) and Transmission Electron Microscopy (TEM), depicted in Figure 4 and Figure 5 at different magnifications, distinctly revealed the two-dimensional nature of graphene and the uniform distribution of ZnS nanoparticles across its surface, observable at both low and high magnifications. Furthermore, the presence of ZnS in the samples was validated through Energy-Dispersive X-ray (EDX) analysis [10].

3.2. Electrochemical activity towards H₂O₂ with G and G/ZnS modified carbon paper electrodes

The determination of hydrogen peroxide (H₂O₂) is crucial due to its importance as an analyte in food, clinical, pharmaceutical, environmental, and industrial analyses, as well as its formation as an electroactive byproduct in enzymatic (ChOx) cholesterol reactions. To investigate the electrochemical response to enzymatically liberated H₂O₂, cyclic voltammetry (CV) was performed using Nafion-ChOx/G and Nafion-ChOx/G-ZnS CP electrodes. Figures 6 and 7 illustrate the cyclic voltammetry (CV)

responses of the respective electrodes. To assess the influence of H₂O₂ on the system, we monitored the alterations in the reduction current following the introduction of 10 μ M H₂O₂ into a 0.1 M phosphate buffer solution at a pH of 7 (refer to Figures 6 and 7). Initially, both electrode configurations exhibited minimal background currents in the absence of H₂O₂. Notably, the ZnS-modified carbon paper (CP) working electrode did not present any observable redox waves, which may be attributed to the semiconducting properties of the metal nanoparticles. Despite the lack of redox activity, the ZnS modification improved the electrical connectivity with the carbon paper electrode when compared to the untreated version. Upon the addition of hydrogen peroxide, the cyclic voltammogram for the G/ZnS-modified electrode exhibited a significant increase in current relative to the ZnS-modified electrode alone. Furthermore, the G/ZnS electrode revealed distinct redox peaks, likely resulting from enhanced electron transport within the G/ZnS/ChOx/NA/CP electrode configuration, in conjunction with the large surface area and high aspect ratio inherent to the nanocomposite material.

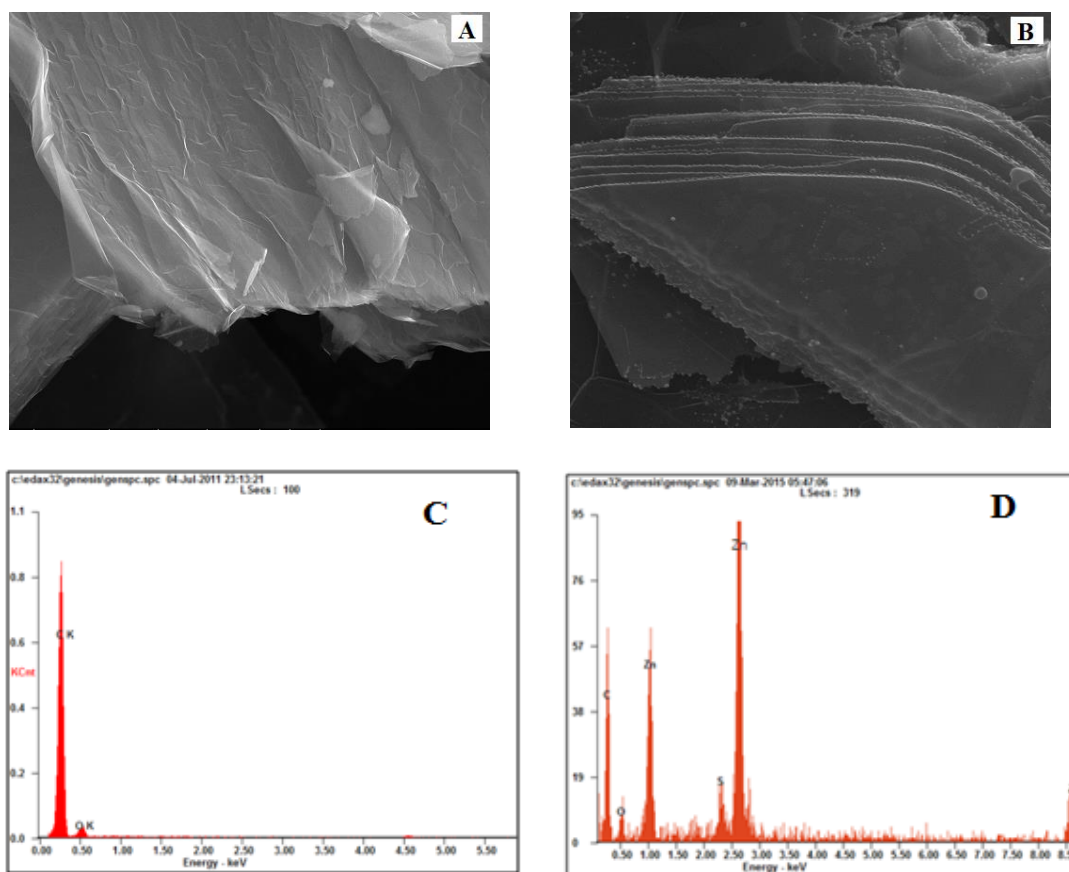


Figure 4. (A), (B) SEM images and (C), (D) EDX of G, G/ZnS, respectively

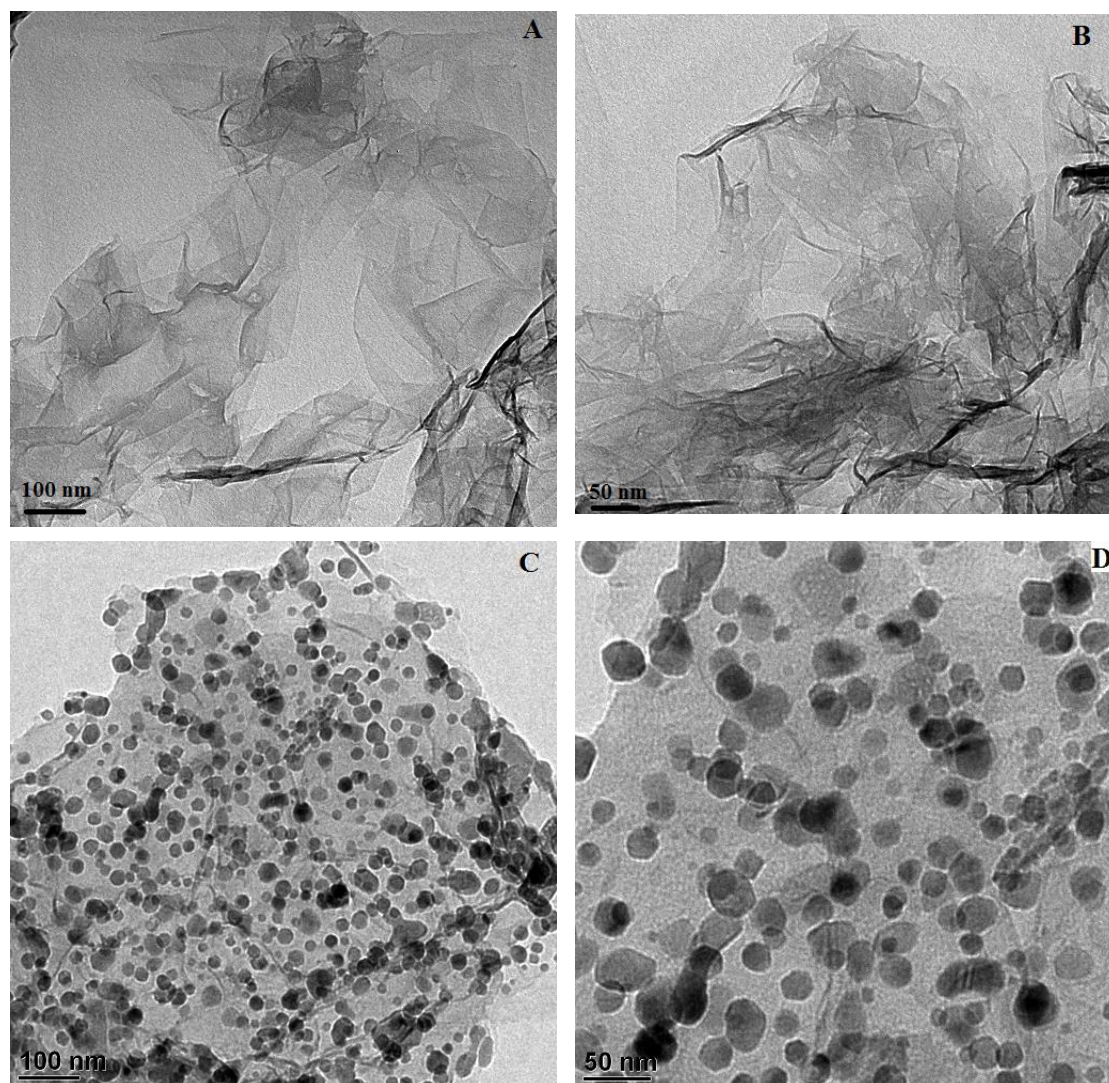


Figure 5. TEM images of Graphene (A ,B) and G/ZnS (C , D), respectively

3.3. Electrochemical activity towards Cholesterol with G and G/ZnS modified carbon paper electrodes

The cholesterol sensor operates through a mechanism based on the selective oxidation of cholesterol by cholesterol oxidase (ChOx). This enzymatic reaction, occurring in the presence of O_2 , generates hydrogen peroxide (H_2O_2). To quantify cholesterol, the probe measures the electrochemical current associated with the oxidation or reduction of this H_2O_2 byproduct. Figures 8 and 9 illustrate the cyclic voltammetry (CV) responses of both G/ChOx/NA/CPE and G/ZnS/ChOx/NA/CPE electrodes upon the addition of $100 \mu M$ cholesterol. These CVs were recorded at scan rates of 25, 50, and 100 mV/s. Compared to a Ag/AgCl reference electrode, the G/ZnS/ChOx/NA/CPE electrode showed characteristic graphene redox peaks. Significantly, the G/ZnS/ChOx/NA/CPE electrode exhibited a greater current response to glucose in phosphate-buffered saline (PBS) than the

ZnS/ChOx/NA/GCE electrode under the same conditions. The well-defined redox peaks in the G/ZnS/ChOx/NA/CPE electrode's CV curve in PBS with $100 \mu M$ cholesterol are attributed to the ChOx-catalyzed oxidation of cholesterol. The large surface area of the G/ZnS nanocomposite facilitates rapid and direct electron transfer between the enzyme ChOx and the electrode surface, leading to these pronounced peaks. Consequently, the G/ZnS/ChOx/CPE electrode effectively senses cholesterol.

3.4. Interference studies

One of the primary difficulties encountered in cholesterol biosensor development is the susceptibility to interference from other biological compounds. Therefore, to evaluate the biosensor's anti-interference performance, electroactive species, specifically uric acid (UA) and ascorbic acid (AA), were introduced. The impact of these potentially interfering species on cholesterol detection at the modified electrode is



depicted in Figure 10. Results indicated that the addition of UA and AA did not cause any discernible increase in the measured current. Collectively, these results underscore the biosensor's robust anti-interference ability.

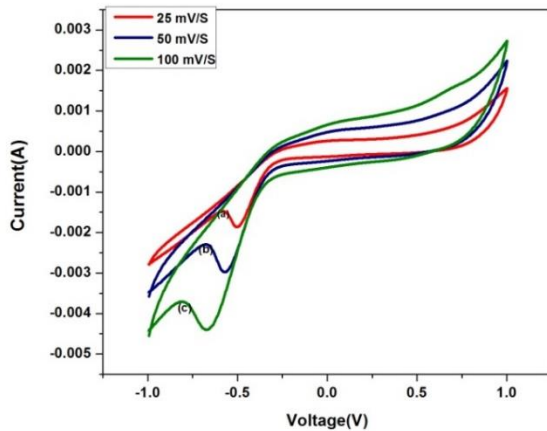


Figure 6. CV of G/ChOx/NA/CPE in 0.01 M PB solution (pH 7.0) containing 0.3 mM H₂O₂ at a scan rate of (a)25 mV/s, (b)50 mV/s and (c)100 mV/s.

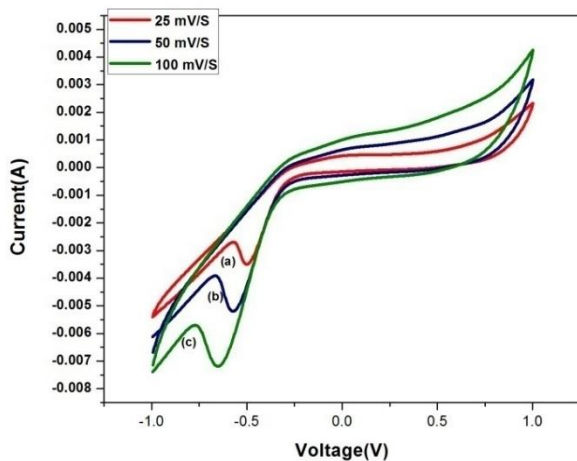


Figure 7. CV of G/ZnS/ChOx/NA/CPE in 0.01 M PB solution (pH 7.0) containing 0.3 Mm H₂O₂ at a scan rate of (a) 25, (b) 50 and (c) 100 mV/s.

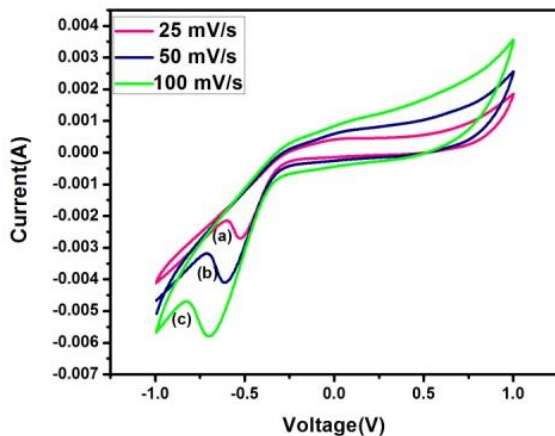


Figure 8. CV of G/ChOx/NA/CPE in 0.1 M PB solution (pH 7) containing 100 μM cholesterol at a scan rate of 25, 50 and 100 mV/s.

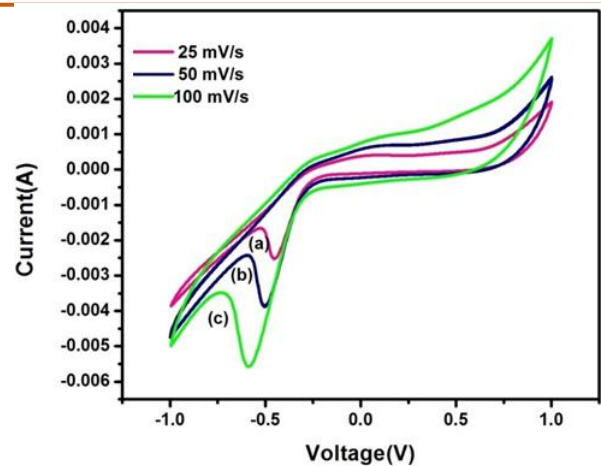


Figure 9. CV of G/ZnS/ChOx/NA/CPE in 0.01 M PB solution (pH 7.0) containing 100 μM cholesterol at a scan rate of 25, 50 and 100 mV/s.

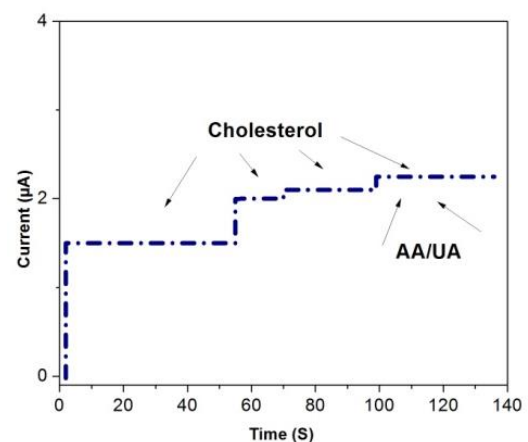


Figure 10. Interference studies of the ZnS/G based cholesterol biosensor by successive addition of ascorbic acid, uric acid and cholesterol, in 0.1 M PB solution (pH 7).

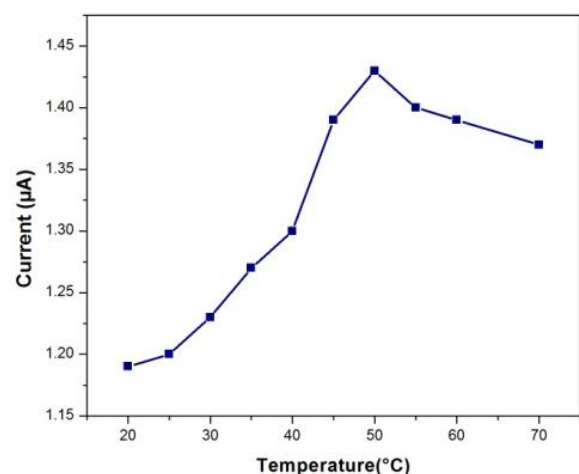


Figure 11. Thermostability of ZnS/G/ChOx/CPE biosensor in PB solution (pH 7) containing 100 μM cholesterol



3.5. Thermostability and pH stability

To assess thermostability, enzyme preparations were pre-incubated with 100 μ M cholesterol for 30 minutes at strain-specific optimum pH across a temperature range of 20–70 $^{\circ}$ C. As temperature increased, the enzymatic activity also increased, leading to a gradual rise in current response that reached its peak at 50 $^{\circ}$ C, as illustrated in Figure 11. As the temperature rose above 50 $^{\circ}$ C, the thermal deterioration of the enzyme led to a steady decline in current response. However, the ZnS/G nanocomposites provided a conducive environment for the immobilized ChOx, which in turn enhanced the thermal stability of the biosensor. This indicates that the ZnS/G biosensor performs best within an operating temperature range of 20 $^{\circ}$ C to 50 $^{\circ}$ C.

Additionally, enzyme activity can affect the pH of cholesterol solutions. To find the ideal operating pH, we assessed the sensor's response to a 100 μ M cholesterol solution at +0.2 V. Figure 12 shows that the biosensor performed optimally within the pH range of 6.0 to 7.1.

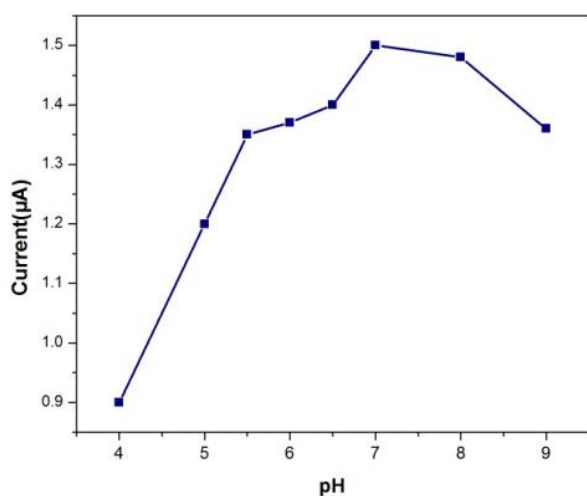


Figure 12. Amperometric response of the ZnS/G/ChOx/CPE biosensor with increasing.

4. Conclusions

The main goal of this research was to create an amperometric cholesterol biosensor by immobilizing cholesterol oxidase (ChOx) onto a ZnS-G nanocomposite working electrode. Leveraging the large surface area and high biocompatibility of the ZnS-G nanocomposites, an optimal environment for the immobilization of chitosan and ChOx was achieved. The resulting biosensor exhibited superior performance in cholesterol detection, characterized by high

sensitivity, a rapid response, excellent long-term stability, and good reproducibility. In conclusion, this study successfully developed a straightforward and highly effective electrochemical method for cholesterol detection, indicating its promising utility in cholesterol biosensing applications.

References

1. A.D. Ambaye, K.K. Kefeni, S.B. Mishra, E.N. Nxumalo, B. Ntsewana, Recent developments in nanotechnology-based printing electrode systems for electrochemical sensors. *Talanta*, 225, (2021) 121951. <https://doi.org/10.1016/j.talanta.2020.121951>
2. M. Baharfar, M. Rahbar, M. Tajik, G. Liu, Engineering strategies for enhancing the performance of electrochemical paper-based analytical devices. *Biosensors and Bioelectronics*, 167, (2020) 112506. <https://doi.org/10.1016/j.bios.2020.112506>
3. A. Kumar, R.R. Pandey, B. Brantley, Tetraethylorthosilicate film modified with protein to fabricate cholesterol biosensor. *Talanta*, 69(3), (2006) 700-705. <https://doi.org/10.1016/j.talanta.2005.11.003>
4. S.K. Arya, P.R. Solanki, R.P. Singh, M.K. Pandey, M. Datta, B.D. Malhotra, Application of octadecanethiol self-assembled monolayer to cholesterol biosensor based on surface plasmon resonance technique. *Talanta*, 69(4), (2006) 918-926. <https://doi.org/10.1016/j.talanta.2005.11.037>
5. E. Solhi, M. Hasanzadeh, P. Babaie, Electrochemical paper-based analytical devices (ePADs) toward biosensing: recent advances and challenges in bioanalysis. *Analytical Methods*, 12(11), (2020) 1398-1414. <https://doi.org/10.1039/D0AY00117A>
6. S.P. Martin, D.J. Lamb, J.M. Lynch, S.M. Reddy, Enzyme-based determination of cholesterol using the quartz crystal acoustic wave sensor. *Analytica Chimica Acta*, 487(1), (2003) 91-100. [https://doi.org/10.1016/S0003-2670\(03\)00504-X](https://doi.org/10.1016/S0003-2670(03)00504-X)
7. A.A. Ansari, A. Kaushik, P.R. Solanki, B.E. Malhotra, Electrochemical cholesterol sensor based on tin oxide-chitosan nanobiocomposite film. *Electroanalysis: An International Journal Devoted to Fundamental and Practical Aspects of Electroanalysis*, 21(8), (2009) 965-972. <https://doi.org/10.1002/elan.200804499>



8. C. Charan, V.K. Shahi, Nanostructured manganese oxide–chitosan-based cholesterol sensor. *Journal of Applied Electrochemistry*, 44, (2014) 953-962. <https://doi.org/10.1007/s10800-014-0704-0>
9. C.C. Allain, L.S. Poon, C.S. Chan, W.F.P.C. Richmond, P.C. Fu, Enzymatic determination of total serum cholesterol. *Clinical chemistry*, 20(4), (1974) 470-475. <https://doi.org/10.1093/clinchem/20.4.470>
10. J.A.T.L. MacLachlan, A.T.L. Wotherspoon, R.O. Ansell, C.J.W. Brooks, Cholesterol oxidase: sources, physical properties and analytical applications. *The Journal of steroid biochemistry and molecular biology*, 72(5), (2000) 169-195. [https://doi.org/10.1016/S0960-0760\(00\)00044-3](https://doi.org/10.1016/S0960-0760(00)00044-3)
11. S. Singh, A. Chaubey, B.D. Malhotra, Preparation and characterization of an enzyme electrode based on cholesterol esterase and cholesterol oxidase immobilized onto conducting polypyrrole films. *Journal of applied polymer science*, 91(6), (2004) 3769-3773. <https://doi.org/10.1002/app.13554>
12. J.C. Vidal, J. Espuelas, J.R. Castillo, Amperometric cholesterol biosensor based on in situ reconstituted cholesterol oxidase on an immobilized monolayer of flavin adenine dinucleotide cofactor. *Analytical biochemistry*, 333(1), (2004) 88-98. <https://doi.org/10.1016/j.ab.2004.06.005>
13. S.K. Arya, P. Pandey, S.P. Singh, M. Datta, B.D. Malhotra, Dithiobissuccinimidyl propionate self assembled monolayer based cholesterol biosensor. *Analyst*, 132(10), (2007) 1005-1009. <https://doi.org/10.1039/B707000D>
14. A. Kumar, R.R. Pandey, B. Brantley, Tetraethylorthosilicate film modified with protein to fabricate cholesterol biosensor. *Talanta*, 69(3), (2006) 700-705. <https://doi.org/10.1016/j.talanta.2005.11.003>
15. S. Brahim, D. Narinesingh, A. Guiseppi-Elie, Amperometric determination of cholesterol in serum using a biosensor of cholesterol oxidase contained within a polypyrrole–hydrogel membrane. *Analytica chimica acta*, 448(1-2), (2001) 27-36. [https://doi.org/10.1016/S0003-2670\(01\)01321-6](https://doi.org/10.1016/S0003-2670(01)01321-6)
16. S. Singh, A. Chaubey, B.D. Malhotra, Amperometric cholesterol biosensor based on immobilized cholesterol esterase and cholesterol oxidase on conducting polypyrrole films. *Analytica chimica acta*, 502(2), (2004) 229-234. <https://doi.org/10.1016/j.aca.2003.09.064>
17. X. Tan, M. Li, P. Cai, L. Luo, X. Zou, An amperometric cholesterol biosensor based on multiwalled carbon nanotubes and organically modified sol-gel/chitosan hybrid composite film. *Analytical Biochemistry*, 337(1), (2005) 111-120. <https://doi.org/10.1016/j.ab.2004.10.040>
18. J.C. Vidal, J. Espuelas, E. Garcia-Ruiz, J.R. Castillo, Amperometric cholesterol biosensors based on the electropolymerization of pyrrole and the electrocatalytic effect of Prussian-Blue layers helped with self-assembled monolayers. *Talanta*, 64(3), (2004) 655-664. <https://doi.org/10.1016/j.talanta.2004.03.038>
19. Z. Matharu, G. Sumana, S.K. Arya, S.P. Singh, V. Gupta, B.D. Malhotra, Polyaniline Langmuir–Blodgett film based cholesterol biosensor. *Langmuir*, 23(26), (2007) 13188-13192. <https://doi.org/10.1021/la702123a>
20. P.R. Solanki, S. Singh, N. Prabhakar, M.K. Pandey, B.D. Malhotra, Application of conducting poly (aniline-co-pyrrole) film to cholesterol biosensor. *Journal of applied polymer science*, 105(6), (2007) 3211-3219. <https://doi.org/10.1002/app.26198>
21. S. Singh, P.R. Solanki, M.K. Pandey, B.D. Malhotra, Covalent immobilization of cholesterol esterase and cholesterol oxidase on polyaniline films for application to cholesterol biosensor. *Analytica Chimica Acta*, 568(1-2), (2006) 126-132. <https://doi.org/10.1016/j.aca.2005.10.008>

Does this article screened for similarity?

Yes

Conflict of interest

The Authors declares that there is no conflict of interest anywhere.

About the License

© The Authors 2024. The text of this article is open access and licensed under a Creative Commons Attribution 4.0 International License.